

# Fatigue Crack Growth

Subjects: **Others**

Contributor: Kailun Wu

The development of crack patterns is a serious problem affecting the durability of orthopedic implants and the prognosis of patients. This issue has gained considerable attention in the medical community in recent years. This literature focuses on the five primary aspects relevant to the evaluation of the surface cracking patterns, i.e., inappropriate use, design flaws, inconsistent elastic modulus, allergic reaction, poor compatibility, and anti-corrosiveness. The hope is that increased understanding will open doors to optimize fabrication for biomedical applications. The latest technological issues and potential capabilities of implants that combine absorbable materials and shape memory alloys are also discussed.

fatigue crack growth    fracture    internal fixation    alloys    absorbable materials

design flaw    elastic modulus    compatibility    allergic reaction

## 1. Introduction

Fatigue crack growth and fracture of orthopedic implants are commonly attributed to the progressive damage under the condition of periodic and intermittent stress load [1]. A sharp increase in the number and size of the micro-cracks is associated with the alternating stress and magnitude of force. When multi-cyclic compression reaches the ultimate tensile strength and as progressive damage accumulates, the internal fixation eventually breaks [2]. The median fatigue limit (MLF) is defined as the minimum load that results in implant failure if exposed to 42,000 cycles, equivalent to about 8 days of walking, on the base of a transverse fracture at the midshaft of femur [3][4]. However, the growth of cracks is a very complicated process in in vivo environments, which are strongly influenced by the biomechanical changes as well as inflammatory response after implantation [5].

Implant failure is usually caused by a network of cracks in the fixation that join and intersect. This network is also referred to as a cracking pattern or as river marks, similar to the branches and small tributaries of a river on a floodplain, as depicted in [Figure 1](#) [6]. River patterns show the direction of fatigue crack progression and are most frequently seen in the relatively fast growing sections of the fatigue zone [7]. The strong correlation between river marks and functional properties of implant allows one to estimate the degree of material degradation. Following Griffith's seminal work [8] concerning a model predicting the crack initiation, subsequent investigators added to the understanding of plasticity [9], toughness [10], and complex geometries [11][12][13]. In orthopedic, fracture mechanics has been exploited to study microstructural damage and energy at the implant-bone interface [14][15]. An important parameter to describe the morphology of the river marks is notch sensitivity, which is given by the fatigue notch

factor (K<sub>f</sub>) [16]. K<sub>f</sub> is the ratio of the fatigue strength of a smooth specimen to that of a notched specimen [17]. The literature provides almost no evidence that the notch sensitivity correlates with the structural integrity of the implant.

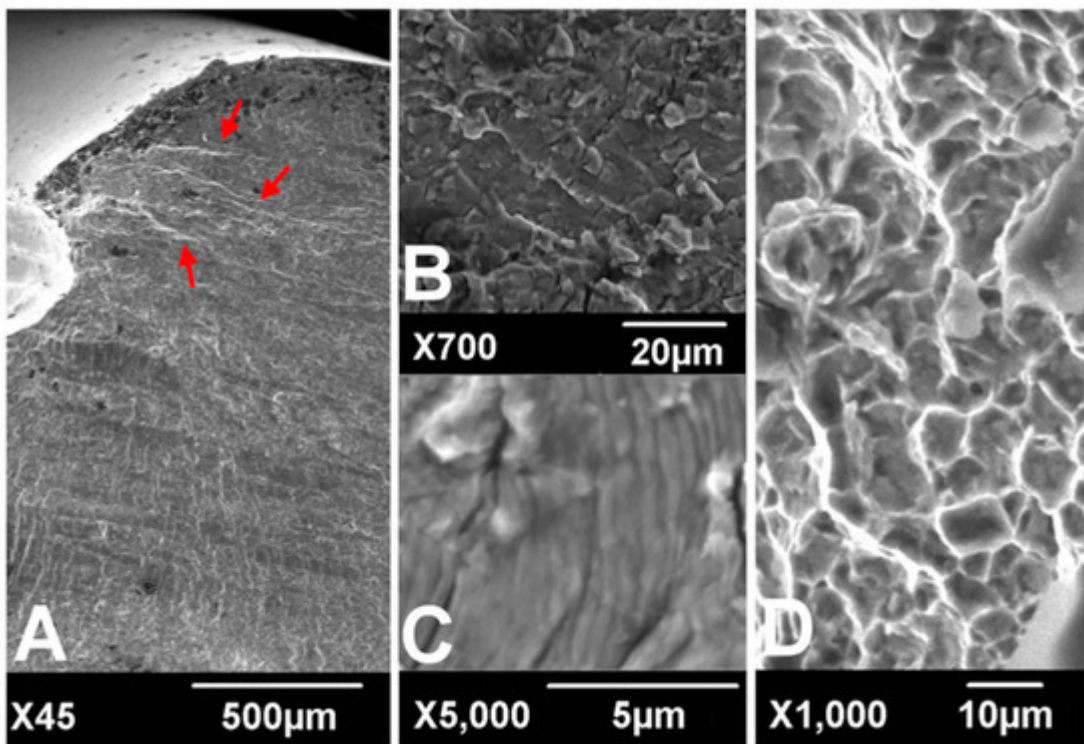


**Figure 1.** Scanning electronic microscopic findings of fracture surfaces. River marks (red arrows) originate from the thread crest (A). Transgranular cracking (B) with striations perpendicular to the river marks (C) was observed at the crack propagation zone. Dimpled ductile fractures were observed at the overload zone (D). (according to [6]).

In terms of biomechanical behavior, the potential hazards of the surrounding soft tissue, blood supply, and severe bone defect play a critical role in the propagation and development of cracks, and their importance has been demonstrated by numerous studies [18][19]. During surgery, the dissection of periosteum and surrounding tissue is inevitable in pursuit of strict fixation and anatomical reduction, which can substantially violate the principle of biological fixation and lead to delayed union and nonunion [19]. Under these circumstances, instability at the fracture site will greatly increase the load acting on the internal fixation. The tension on the implanted device can also be created by repeated bending stress. The duration of excessive load and impact, meanwhile, will increase the longer it takes for the bone fracture to heal [20].

The analysis of crack growth draws on many fields of science, including the biomechanical effect, fracture mechanics, image analysis, and materials engineering [21]. Despite advances in theory and surgical techniques, the risk mitigation of fixation failure resulting from biomechanical effects is still in its early stages. At least, technical solutions are reaching a crossroad on this point. Consequently, the latest publication on the applicability of materials has been thrust into the limelight as we strive to lower the incidence of fatigue crack growth [22][23][24]. Currently, stainless steel, titanium (Ti), and cobalt-chromium (Co-Cr) alloy are the major materials used for the fabrication of the orthopedic inner fixing apparatus [25]. In international clinical practice, the most widely used

medical stainless steel materials for surgical implant are austenitic stainless steel-316L, 317L, etc. [1]. Starting with austenitic stainless steel, titanium is added to make the material more resistant to corrosion, increase fatigue strength, lower infection risk, and improve the isoelasticity of bones, Ti-6Al-4V is the most frequently used titanium alloy for biomedical application [26]. Hardness is principally improved by adding molybdenum and through the reduction of sulfur, phosphorus, and other impurities [27][28]. The dominant properties of nickel-free nitrogen-containing stainless steel are rust resistance and toughness, which make the materials adapt better to the biochemical environment *in vivo* [29].

## 2. Inappropriate Use of Internal Fixation

### 2.1. Reshaping of Internal Fixation

Currently, internal fixation still does not match the anatomy of human skeleton perfectly [34]. To remedy the situation, plates are often bent repeatedly to fit snugly onto the bone surface during the aesthetic procedure. Unfortunately, this reshaping can greatly decrease the strength of the plate and speed up the erosion of metal, a primary reason for cracking. At this point, pores close to the surface will become nuclei for fatigue cracks [35]. Subsequently, a sudden release of elastic energy effortlessly can cause the local tensile strength of the nail to be exceeded, resulting in acute failure. Indeed, in plate bending, although the compressed threads tend to disperse minimal stress concentration effect, hole threads still can act as notches and diminish the fatigue strength even with minimal stress intensity, especially in titanium devices [6]. The fatigue strength may also be impacted by bending frequencies, displaying an obviously positive correlation [36]. It has been reported that the fatigue resistance of bending could be enhanced by exerting a sufficient compressive stress on the implant surface and reducing the crystallite size, which has been realized through sandblasting [37]. According to the operation specification, it is strictly forbidden to bend the site of a screw hole, in order to maintain the mechanical strength of steel counterpart. Slight bending between threaded holes is permitted if necessary. Fortunately, these configurational incongruities may be perfectly tackled by customization via 3D printing to enhance implants' survivorship of fracture fixation in the short run [38].

### 2.2. Interaction of the Different Materials

A sandwich of two different metals can induce a continuous micro-current (a.k.a galvanic corrosion) [39]. A similar situation arises with internal fixation *in vivo*. In clinical practice, the fixations made from different material compositions may have to be selected in view of a lack of matching apparatus or using stainless wire to tie up bone fragments. Despite the fact that a stable oxide film between the high-quality metals is expected to suppress galvanic corrosion in theory, it was still reported in the literature that a micro-current between the plate and screws can cause electrolytic corrosion and substantially decrease the strength of fixation [40][41].

Besides, in the case of the implants with unstable fixation, scratch and friction damage of the oxide film have been detected at the interface, which could explain why galvanic corrosion occurred [42]. Depending on the electrolyte solution *in vivo*, the passive oxide film may undergo a cycle of the dissociation and re-oxidation, where the absence

of the dissolved oxygen dramatically hampers the repair of the oxide film. Regarding stainless steel, electrolytic corrosion often appears as pit corrosion due to the perforation from chlorine ions, or crevice corrosion as a result of the inhomogeneous distribution of the dissolved oxygen [43]. The primary factors influencing the strength of the galvanic coupling are not only the corrosion potential difference caused by composition of each constituent phase but also the effective contact area of Cathode/Anode. Therefore, weak galvanic corrosion may take place even at the interface between the identical alloys, at least in theory, attributed to minor differentials in the impurity distribution. Fatigue crack initiation can take place at the base of galvanic corrosion. Thereafter, the crack initiation shifts towards the shoulder and the mouth of the pit as the depth of the corroded site increases [44].

## 2.3. The Weakest Link of Internal Fixation

It is extensively known that the hole structure is the weakest link of the fixation [31]. If the weakest links are placed in the vicinity of a fracture, the local stress will be concentrated on the transitional sites, which may be capable of destroying the structure of the plate near the crack limit [4]. In short, an implant is only as strong as its weakest link. As an evidence of the propagation of fatigue cracks in a locking compression plate (LCP), the striations or fatigue cracks are seen first to initiate from a subsurface inclusion embedded under the surface of compression hole and the surface of the locking hole. Once cracks are initiated, the residual stress and microstructure affect the fatigue crack growth [45]. Then both cracks propagate inside the plate [4]. Moreover, it has also been observed that the thread crest is subjected to a maximal stress under bending load and has a tendency to be the fatigue crack initiation site [6]. Kanchanomai et al. found that the propagation of cracks from the initiation site to the bottom part of plate required nearly 5000 cycles in fatigue tests [4]. It is therefore necessary to choose a plate with even numbered holes or without center holes, so as to avoid placing the middle hole on top of the fracture site.

According to the work by Lin et al., the modification of screw hole structures can improve the fatigue strength of plate effectively by removing the threads at the tension side and increasing the crest radii of the threads ([Figure 2](#)) [6]. It was also reported that locking buttons were utilized to plug the empty holes adjacent to a defect, that could be implemented to increase the fatigue strength and fatigue life by 4 times compared with plates with unfilled holes ([Figure 3](#)) [46][47][48]. The usage of two buttons for locking raised the survival probability. However, the authors did not to date test the strength of the construct adjacent to the fracture site for using a single button or in Long-span comminuted fracture. Further studies, especially including the fatigue crack propagation of the LCP engaged by locking buttons, will be necessary to better predict the fatigue life of an implant in a given clinical situation.

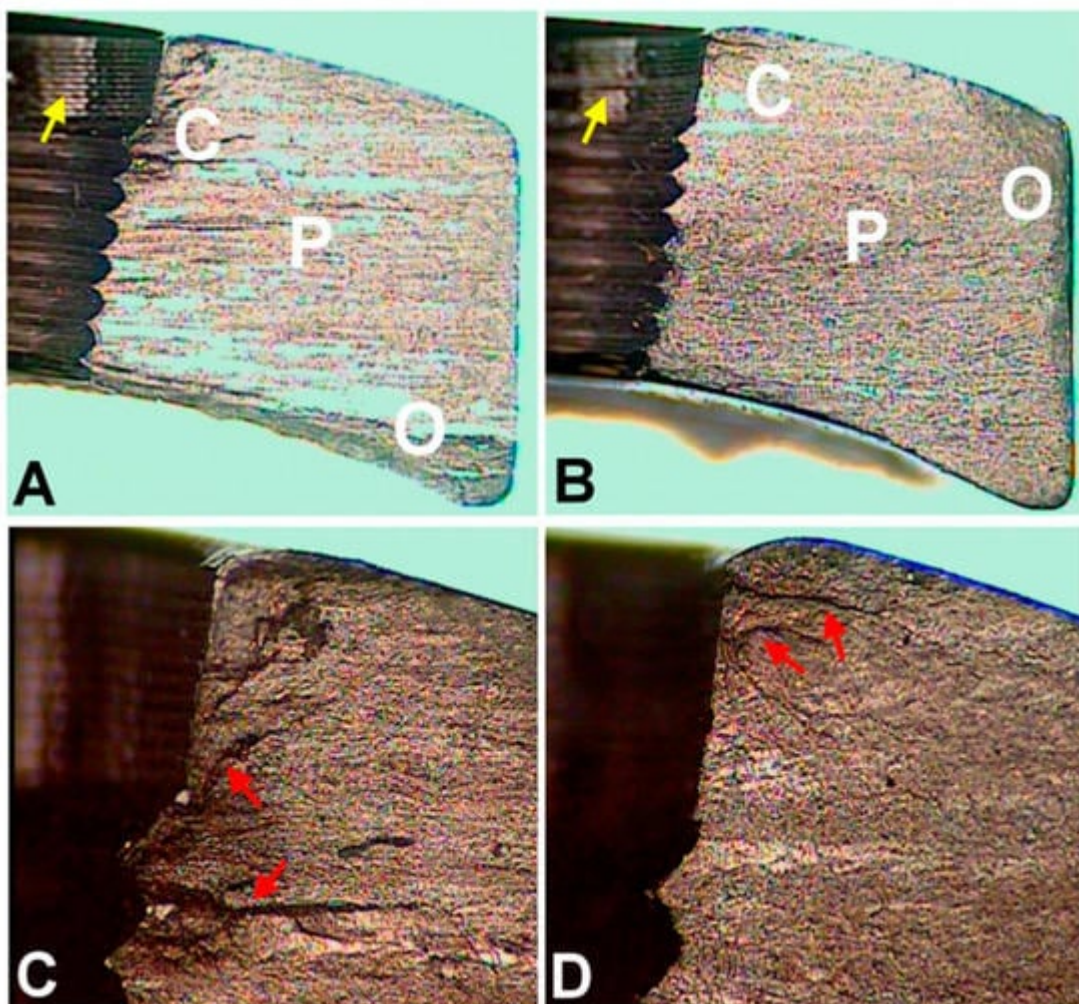


**Figure 2.** Optical microscopic images of fracture surfaces. There are three zones indicating fatigue fracture (**A,B**) and the magnified views of the crack initiation sites (**C,D**). C represents the crack initiation zone. P represents the crack propagation zone. O represents the final overloading zone. Red arrows point to the crack lines. Yellow arrows point to the machining lines at the screw holes. (according to [6]).

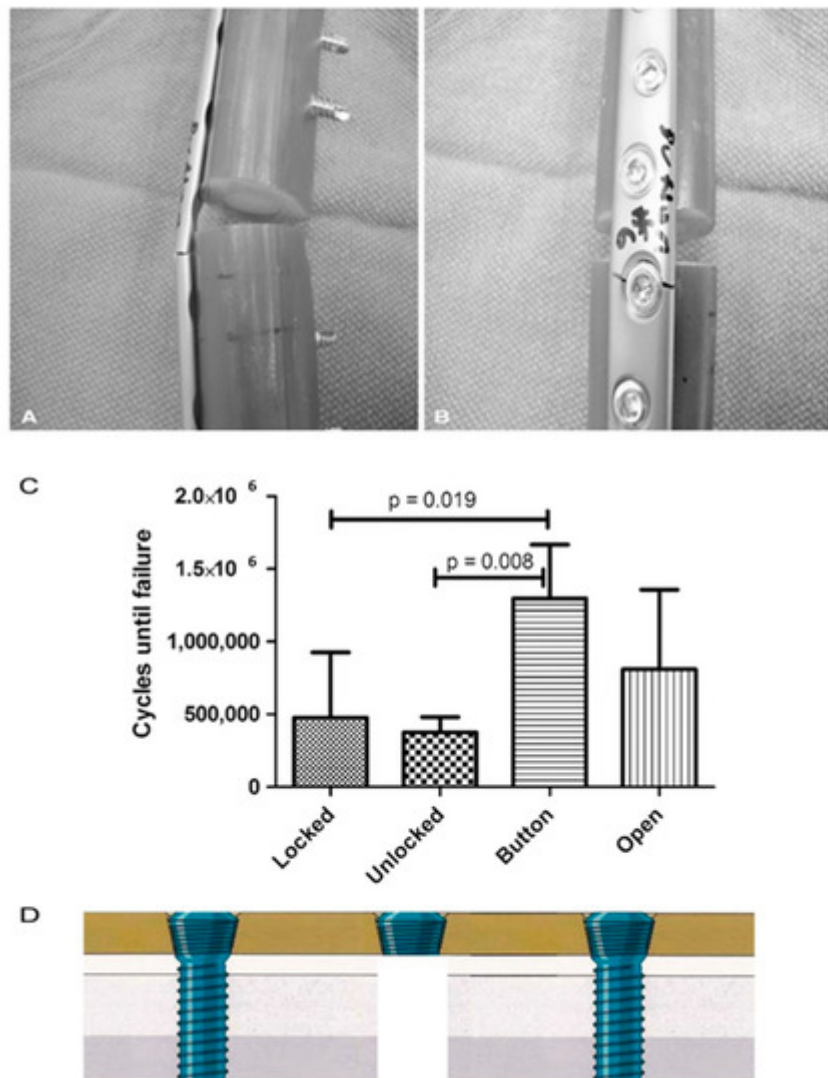


**Figure 3.** (A,B) All plates failed through a screw hole adjacent to the defect as is seen on the (A) left and (B) right in these representative Button samples. (C) The fatigue life in cycles to failure is shown for each plate and screw configuration. (according to [46]). (D) The authors did not to date test the strength of the construct near the fracture site for using a single button.

### 3. Design Flaws of Internal Fixation

Design flaws are a key reason for fatigue crack growth in internal fixation [49]. Take the case of intramedullary nail. The design of tubular intramedullary nailing cannot provide a large amount of transverse elastic space depending on the need for weight-bearing exercise. Accordingly, the nail has to be placed under low resistance in the practice of medullary nail due to its transverse fragility [50]. Moreover, broken interlocking screws can be found more frequently if small-diameter nails are used [51]. Semeer and colleagues speculated that vibration of such slightly loose nails in the canal may corrode the bolt at the nail-bolt interface and ultimately lead to further bolt weakening and the emergence of cracks [52]. Therefore, we recommend a nail, which is 1.0 to 1.5 mm smaller than the

ultimate size of intramedullary reaming in practice. Otherwise, the split of diaphysis and deformation of the intramedullary nail may easily commence when the nail is hammered into the coarser medullary cavity by force [53].

For the treatment of fracture, blood supply and stability are prerequisites for fracture union, and the axial interfragmentary motorization can expedite the course of bone remodeling [54][55]. However, untimely dynamization gives rise to a range of disastrous complications, such as limb shortening, deformity of rotation, and nonunion [56]. In order to take this into account, early dynamization is recommended, unless the fracture still manifests no signs of healing three months after treatment with interlocking intramedullary nails or a comminuted fracture is identified [57]. With regard to unstable fracture configuration, internal fixation could not ensure stability with low anti-torsion capacity and poor shear strength on the vertical axis after being changed into dynamic fixation, in spite of compressing the fracture end. The main factors contributing to this phenomenon incorporate the traction of muscle and resorption of the fracture end [57]. To cope with this, Dailey et al. have proposed a novel intramedullary nail design, which can generate a stimulatory micro-motion under minimal weight-bearing loads on the strength of cadaver observation (Figure 4) [54]. In the future, an analogous design may secure a dominant position on medical-instrumentation platforms.

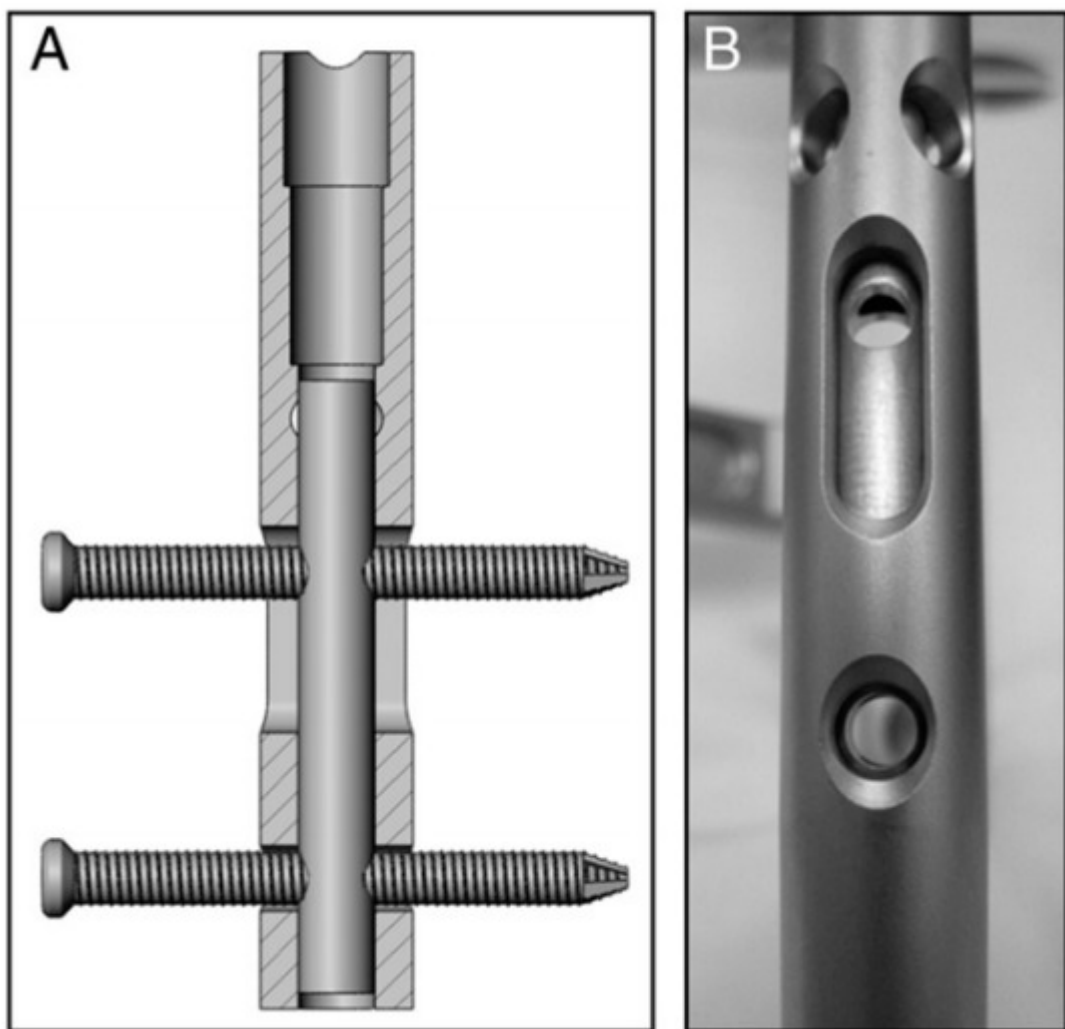


**Figure 4. (A,B)** Prior to implantation of the nails, a micromotion insert was placed in the proximal cannulus of each nail. An insert in the proximal nail stem was used to align two 3.9-mm locking bolts—one in the dynamic slot and one in the 5-mm static locking hole. This configuration produced 1.1 mm of free axial travel (according to [54]).

In the case of middle and distal tibia fracture, the intramedullary nail ought to be implanted into the distal side of cancellous bone below the isthmus. However, the distal portion of intramedullary nail is usually difficult to anchor depending on open cancellous bone [50]. It means that the tip of intramedullary nail is easy to move around or impact medial wall of bone cortex, and this eventually causes a fatigue crack or break in the implant. Hence, this imperfection of design has to be overcome by using blocking screws, which in a sense can limit the wiggle of the tip by guaranteeing the length of the nail [58].

## 4. Biological Compatibility and Corrosiveness of Implants

Sustaining multiaxial loading, including tension, compression, bending, and torsion, is one prime challenge of implants which also must survive in a very corrosive medium *in vivo* (high concentrations of enzymes, proteins, salts) [68]. Subject to this cooperative attack, load-bearing implants are prone to corrosion and some inevitable level of wear and tear [69]. It is a fact that corrosion resistance is adequate even in the presence of cracks, but not necessarily once a dynamic load is exerted. This can bring about the irreversible breakage of the passivation layer so that the metal ions spread towards the surrounding tissue.

Compound interactions, like ion exchange or adsorption of proteins, determine the quality and stability of the bone-implant-interface [70]. These redox-reactions may cause conformational variations of biological macromolecules transforming native proteins into antigens which notify the immunological system to recognize an artificial implant as a foreign body [71]. Besides, the surface of the implant can become a fascinating battleground for the spontaneous degeneration and infiltration with inflammatory cells [72][73]. The degradation products are in turn liable to incite aseptic inflammation. The former can produce toxic side-effects, while the later can lead to a total loss of material cohesion [74]. Some relevant studies have conducted a deep analysis of the stress intensity threshold for fatigue ( $K_{max,th}$ ) in corrosive media [75]. The results indicated that corrosive environment possesses a time-dependent attribute, contributing to fatigue crack growth even when stress intensity factor ( $K_{max}$ ) is less than stress intensity threshold for stress corrosion cracking ( $K_{Iscc}$ ) ([Figure 5](#)).

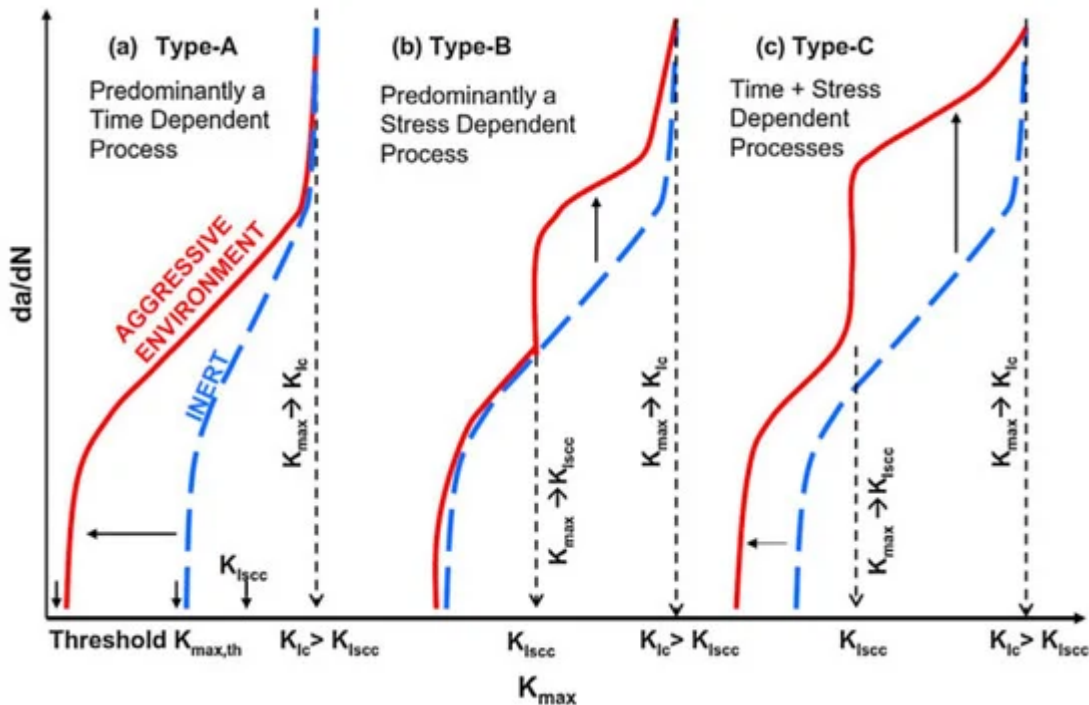


**Figure 5.** Schematic representation of crack growth under different scenarios of simultaneous cyclic and tensile loading in inert and corrosive environment (according to [25]).

Generally, the surface will experience four different corrosion phases, namely immunity, active metal dissolution, passivity, and transpassive metal dissolution [26]. The surface is defined as the electrochemical context where a strongly adherent surface oxide film of a 2–10 nm thickness is present [27]. On the one hand, such an oxide film reduces the dissolution rate of the metal by acting as a physical barrier limiting the transport of electrons, cations and anions between the metal and the electrolyte, and reducing the kinetics of the anodic and cathodic reactions underlying the corrosion process. On the other hand, the deposition of oxide or nitride particles could induce the adherence of tissue to the rough surface of implant, as depicted in [Figure 6](#) [28]. The thickness of the passive film on alloys and its composition changes with potential [27]. The actual value of the corrosion potential is determined by the relative velocities of the formation of novel surface modification and its repassivation [29]. The velocity of the repassivation itself depends on the kinetics of the metal surface reactions and the conditions for oxygen access. However, the repassivation of a mechanically impaired surface areas is hardly possible in the oxygen-deficient medium so any fatigue crack advances faster.

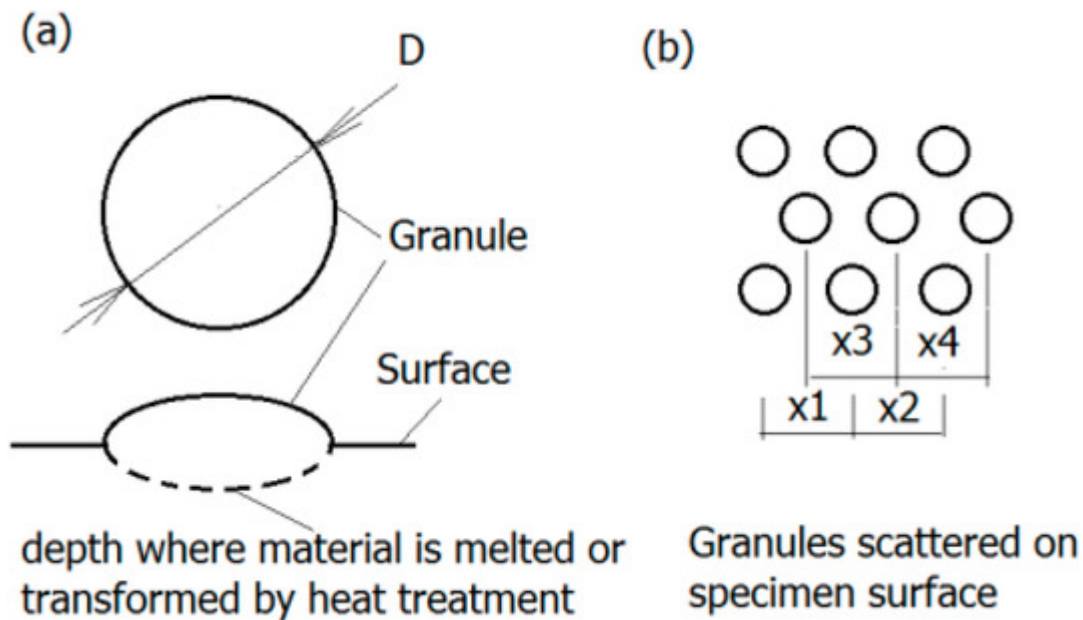


**Figure 6.** Granular surface: (a) Geometry of granules—The region of melted and transformed material is marked dashed line; (b) granules displacement on the surface (according to [78]).

Titanium and its alloys form a very stable oxide layer in quasi-physiological environments bestowing them with exceptional biocompatibility as compared to other metal implant materials [80]. Pitting and crevice corrosion have scarcely been found on implants of Ti-alloys up until now [81]. Their interfacial reaction products predominantly consist of anatase and rutile ( $\text{TiO}_2$ ) represented by a tetragonal lattice structure [71]. In contrast to the ion-conducting passive films formed on stainless steel or cobalt and nickel-based alloys, Ti forms a semi-conducting passive layer. A further property of the layer is the regeneration of the oxide layer in milliseconds even after damage in poorly oxygenated media. Depending on the phases that can be retained at room temperature, Ti alloys are classified into three categories:  $\alpha$ ,  $\alpha+\beta$ , and metastable  $\beta$  alloys [82]. According to a recent investigation, corrosion attack in  $\alpha/\beta$  Ti alloys often initiates at the  $\alpha/\beta$  interfaces, as multi-step process [83]. Furthermore, it has also been documented in the literature that the different rates of film formation on the  $\alpha$  and  $\beta$  phases can cause film fracture at  $\alpha/\beta$  interfaces thereby initiating corrosion attack [82]. Moreover, based on the theory by Slámečka et al., the size, scatter, and depth of oxide granules on the implant surface may affect the fatigue resistance greatly by acting as crack initiation sites [84]. The formation and growth of a fatigue crack is more likely if the mechanical properties of the oxide layer and implant are of considerable discrepancy [85]. Therefore, the oxide layer can be either a defender or a security risk for internal fixation.

## References

1. Sivakumar, M.; Rajeswari, S. Investigation on biomechanically induced fatigue failure of a stainless steel orthopaedic implant device. *J. Mater. Sci. Lett.* 1993, 12, 145–148.

2. Kandemir, U.; Augat, P.; Dipl.-Ing, S.K.; Dipl.-Ing, F.W.; Geert, D.I.; Schmidt, U. Implant Material, Type of Fixation at the Shaft, and Position of Plate Modify Biomechanics of Distal Femur Plate Osteosynthesis. *J. Orthop. Trauma* 2017, 31, e241–e246.
3. Varady, P.A.; von Ruden, C.; Greinwald, M.; Hungerer, S.; Patzold, R.; Augat, P. Biomechanical comparison of anatomical plating systems for comminuted distal humeral fractures. *Int. Orthop.* 2017, 41, 1709–1714.
4. Kanchanomai, C.; Phiphobmongkol, V.; Muanjan, P. Fatigue failure of an orthopedic implant—A locking compression plate. *Eng. Fail. Anal.* 2008, 15, 521–530.
5. Bundy, K.J.; Marek, M.; Hochman, R.F. In vivo and in vitro studies of the stress-corrosion cracking behavior of surgical implant alloys. *J. Biomed. Mater. Res.* 1983, 17, 467–487.
6. Lin, C.H.; Chao, C.K.; Ho, Y.J.; Lin, J. Modification of the screw hole structures to improve the fatigue strength of locking plates. *Clin. Biomech. (Bristol, Avon)* 2018, 54, 71–77.
7. Neville, W.S.P.E. Understanding the surface features of fatigue fractures: How they describe the failure cause and the failure history. *J. Fail. Anal. Prev.* 2005, 5, 11–15.
8. Griffith, A.A. The Phenomena of Rupture and Flow in Solids. *Philos. Trans. R. Soc. Lond.* 1921, 221, 163–198.
9. Arriaga, M.; Waisman, H. Stability analysis of the phase-field method for fracture with a general degradation function and plasticity induced crack generation. *Mech. Mater.* 2018, 116, 33–48.
10. Cuenca, E.; Ferrara, L. Fracture toughness parameters to assess crack healing capacity of fiber reinforced concrete under repeated cracking-healing cycles. *Theor. Appl. Fract. Mech.* 2019, 106, 102468.
11. Li, J.; Leguillon, D. Finite element implementation of the coupled criterion for numerical simulations of crack initiation and propagation in brittle materials. *Theor. Appl. Fract. Mech.* 2018, 93, 105–115.
12. Macek, W.; Branco, R.; Szala, M.; Marciniak, Z.; Ulewicz, R.; Sczygiol, N.; Kardasz, P. Profile and Areal Surface Parameters for Fatigue Fracture Characterisation. *Materials* 2020, 13, 3691.
13. Macek, W.; Branco, R.; Trembacz, J.; Costa, J.D.M.; Capela, C.A. Effect of multiaxial bending-torsion loading on fracture surface parameters in high-strength steels processed by conventional and additive manufacturing. *Eng. Fail. Anal.* 2020, 118, 104784.
14. Durn, J.A.R.; Castro, J.T.P.; Filho, J.C.P. Fatigue crack propagation prediction by cyclic plasticity damage accumulation models. *Fatigue Fract. Eng. Mater. Struct.* 2003, 26, 137–150.
15. Damm, N.B.; Morlock, M.M.; Bishop, N.E. Friction coefficient and effective interference at the implant-bone interface. *J. Biomech.* 2015, 48, 3517–3521.

16. Hosseini, S.; Limooei, M.B. Investigation of Fatigue Behaviour and Notch Sensitivity of Ti-6Al-4V. *Appl. Mech. Mater.* 2011, 80–81, 7–12.
17. Cheng, Z.; Liao, R.; Lu, W.; Wang, D. Fatigue notch factors prediction of rough specimen by the theory of critical distance. *Int. J. Fatigue* 2017, 104, 195–205.
18. von Rüden, C.; Augat, P. Failure of fracture fixation in osteoporotic bone. *Injury* 2016, 47, S3–S10.
19. Kwang-Bok, L.; Seong-Yup, J.; Seung-Ho, K.; Dong-Gun, S. Complete Reduction for Pilon Fracture Can Make Complete Failure. *J. Am. Podiatr. Med. Assoc.* 2018, 108, 257–261.
20. Stern, J.K.; Hahn, E.E.; Evian, C.I.; Waasdorp, J.; Rosenberg, E.S. Implant failure: Prevalence, risk factors, management, and prevention. In *Dental Implant Complications: Etiology, Prevention, and Treatment*, 2; Stuart, J., Froum, D.D.S., Eds.; John Wiley & Sons, Ltd: Hoboken, NJ, USA, 2015; pp. 153–169.
21. Mughrabi, H. Microstructural mechanisms of cyclic deformation, fatigue crack initiation and early crack growth. *Philos. Trans. R. Soc. A Philos. Trans. Ser. A Math. Phys. Eng. Sci.* 2015, 373, 20140132.
22. Singh Raman, R.K.; Jafari, S.; Harandi, S.E. Corrosion fatigue fracture of magnesium alloys in bioimplant applications: A review. *Eng. Fract. Mech.* 2015, 137, 97–108.
23. Li, F.; Li, J.; Huang, T.; Kou, H.; Zhou, L. Compression fatigue behavior and failure mechanism of porous titanium for biomedical applications. *J. Mech. Behav. Biomed. Mater.* 2017, 65, 814–823.
24. Bonnheim, N.; Ansari, F.; Regis, M.; Bracco, P.; Pruitt, L. Effect of carbon fiber type on monotonic and fatigue properties of orthopedic grade PEEK. *J. Mech. Behav. Biomed. Mater.* 2018, 90, 484–492.
25. Gotman, I. Characteristics of Metals Used in Implants. *J. Endourol.* 1998, 11, 383–389.
26. Hayes, J.S.; Richards, R.G. The use of titanium and stainless steel in fracture fixation. *Expert Rev. Med. Devices* 2010, 7, 843–853.
27. Rahman, T.; Ebert, W.L.; Indacochea, J.E. Effect of molybdenum additions on the microstructures and corrosion behaviours of 316L stainless steel-based alloys. *Corros. Eng. Sci. Technol.* 2018, 53, 226–233.
28. Kimura, T.; Iwasaki, S.; Sakuraya, K.; Tanuma, S. The Quantitative Analysis of Super-Low Phosphorus Content of SUS316L Type Stainless Steel With EPMA Calibration Curve Method. *Microsc. Microanal.* 2008, 14, 1136–1137.
29. Talha, M.; Behera, C.K.; Sinha, O.P. A review on nickel-free nitrogen containing austenitic stainless steels for biomedical applications. *Mater. Sci. Eng. C-Mater. Biol. Appl.* 2013, 33, 3563–3575.

30. Hsu, C.C.; Yongyut, A.; Chao, C.K.; Lin, J. Notch sensitivity of titanium causing contradictory effects on locked nails and screws. *Med. Eng. Phys.* 2010, 32, 454–460.

31. Tseng, W.J.; Chao, C.K.; Wang, C.C.; Lin, J. Notch sensitivity jeopardizes titanium locking plate fatigue strength. *Injury* 2016, 47, 2726–2732.

32. Dimic, I.; Cvijović-Alagić, I.; Rakin, M.; Branko, B. Analysis of metal ion release from biomedical implants. *Metall. Mater. Eng.* 2013, 19, 167–176.

33. Thelen, S.; Barthelat, F.; Brinson, L. Mechanics considerations for microporous titanium as an orthopedic implant material. *J. Biomed. Mater. Res. Part A* 2004, 69, 601–610.

34. Wu, K.; Su, X.; Roche, S.J.L.; Held, M.F.G.; Yang, H.; Dunn, R.N.; Guo, J.J. Relationship between the lateral acromion angle and postoperative persistent pain of distal clavicle fracture treated with clavicle hook plate. *J. Orthop. Surg. Res.* 2020, 15, 217.

35. Leuders, S.; Thoene, M.; Riemer, A.; Niendorf, T.; Troester, T.; Richard, H.A.; Maier, H.J. On the mechanical behaviour of titanium alloy TiAl6V4 manufactured by selective laser melting: Fatigue resistance and crack growth performance. *Int. J. Fatigue* 2013, 48, 300–307.

36. Liu, Y.J.; Cui, S.M.; He, C.; Li, J.K.; Wang, Q.Y. High cycle fatigue behavior of implant Ti-6Al-4V in air and simulated body fluid. *Biomed. Mater. Eng.* 2014, 24, 263–269.

37. Balza, J.C.; Zujur, D.; Gil, L.; Subero, R.; Dominguez, E.; Delvasto, P.; Alvarez, J. Sandblasting as a surface modification technique on titanium alloys for biomedical applications: Abrasive particle behavior. *IOP Conf. Ser. Mater. Sci. Eng.* IOP Publ. 2013, 45, 012004.

38. Yan, L.; Lim, J.L.; Lee, J.W.; Tia, C.S.H.; O'Neill, G.K.; Chong, D.Y.R. Finite element analysis of bone and implant stresses for customized 3D-printed orthopaedic implants in fracture fixation. *Med. Biol. Eng. Comput.* 2020, 58, 921–931.

39. Bhola, R.; Bhola, S.M.; Mishra, B.; Olson, D.L. Corrosion in titanium dental implants/prostheses—A review. *Trends Biomater. Artif. Organs* 2011, 25, 34–46.

40. Okazaki, Y. Galvanic Corrosion Properties of a Highly Biocompatible Ti-15Zr-4Nb-4Ta alloy. *Jpn. J. Clin. Biomech.* 2010, 31, 213–217.

41. Virtanen, S.; Milosev, I.; Gomez-Barrena, E.; Trebse, R.; Salo, J.; Konttinen, Y.T. Special modes of corrosion under physiological and simulated physiological conditions. *Acta Biomater.* 2008, 4, 468–476.

42. Kato, Y.I.A.; Hattori, T.; Akahori, T.; Kimata, N.; Sato, K. Animal Experiment on In vivo Galvanic Corrosion of SUS316L and Ti-6Al-4V. *J. Mater. Sci. Eng.* 2015, 4, 1000156.

43. Brown, S.A.; Simpson, J.P. Crevice and fretting corrosion of stainless-steel plates and screws. *J. Biomed. Mater. Res.* 2010, 15, 867–878.

44. Co, N.E.C.; Burns, J.T. Galvanic Corrosion-Induced Fatigue Crack Initiation and Propagation Behavior in AA7050-T7451. *Corrosion* 2016, 72, 1215–1219.

45. Kasperovich, G.; Hausmann, J. Improvement of fatigue resistance and ductility of TiAl6V4 processed by selective laser melting. *J. Mater. Process. Technol.* 2015, 220, 202–214.

46. Tompkins, M.; Paller, D.J.; Moore, D.C.; Crisco, J.J.; Terek, R.M. Locking buttons increase fatigue life of locking plates in a segmental bone defect model. *Clin. Orthop. Relat. Res.* 2013, 471, 1039–1044.

47. Bellapianta, J.; Dow, K.; Pallotta, N.A.; Hospodar, P.P.; Uhl, R.L.; Ledet, E.H. Threaded screw head inserts improve locking plate biomechanical properties. *J. Orthop. Trauma* 2011, 25, 65–71.

48. Zhang, J.Y.; Tornetta, P., 3rd; Jones, B.; Zheng, Y.; Whitten, A.; Cartner, J.; Ricci, W.M. Locking Hole Inserts: Effect of Insertion Torque on Fatigue Performance and Insert Loosening in Locking Plates. *J. Orthop. Trauma* 2019, 33, 120–124.

49. Guerra-Fuentes, L.; Garcia-Sanchez, E.; Juarez-Hernandez, A.; Hernandez-Rodriguez, M.A.L. Failure analysis in 316L stainless steel supracondylar blade plate. *Eng. Fail. Anal.* 2015, 57, 243–247.

50. Serrano, R.; Mir, H.R.; Karsch, J.; Kim, R.; Sanders, R.W. Effect of Nail Size, Insertion, and  $\Delta$  Canal-Nail on the Development of a Nonunion After Intramedullary Nailing of Femoral Shaft Fractures. *J. Orthop. Trauma* 2019, 33, 1.

51. Weninger, P.; Schueller, M.; Jamek, M.; Stanzl-Tschegg, S.; Redl, H.; Tschegg, E.K. Factors influencing interlocking screw failure in unreamed small diameter nails--a biomechanical study using a distal tibia fracture model. *Clin. Biomech.* 2009, 24, 379–384.

52. Aggerwal, S.; Gahlot, N.; Saini, U.C.; Bali, K. Failure of intramedullary femoral nail with segmental breakage of distal locking bolts: A case report and review of the literature. *Chin. J. Traumatol. (Engl. Ed.)* 2011, 14, 188–192.

53. Wu, K.; Xu, Y.; Zhang, L.; Zhang, Y.; Guo, J.J. Which implant is better for beginners to learn to treat geriatric intertrochanteric femur fractures: A randomised controlled trial of surgeons, metalwork, and patients. *J. Orthop. Transl.* 2019, 21, 18–23.

54. Dailey, H.L.; Daly, C.J.; Galbraith, J.G.; Cronin, M.; Harty, J.A. A novel intramedullary nail for micromotion stimulation of tibial fractures. *Clin. Biomech. (Bristol, Avon)* 2012, 27, 182–188.

55. Ma, Y.G.; Hu, G.L.; Hu, W.; Liang, F. Surgical factors contributing to nonunion in femoral shaft fracture following intramedullary nailing. *Chin. J. Traumatol.* 2016, 19, 109–112.

56. Schultz, B.J.; Koval, K.; Salehi, P.P.; Gardner, M.J.; Cerynik, D.L. Controversies in Fracture Healing: Early Versus Late Dynamization. *Orthopedics* 2020, 43, e125–e133.

57. Perumal, R.; Shankar, V.; Basha, R.; Jayaramaraju, D.; Rajasekaran, S. Is nail dynamization beneficial after twelve weeks—An analysis of 37 cases. *J. Clin. Orthop. Trauma* 2017, 9, 322–326.

58. Chan, D.S.; Nayak, A.N.; Blaisdell, G.; James, C.R.; Denard, A.; Miles, J.; Santoni, B.G. Effect of distal interlocking screw number and position after intramedullary nailing of distal tibial fractures: A biomechanical study simulating immediate weight-bearing. *J. Orthop. Trauma* 2015, 29, 98–104.

59. Head, W.C.; Bauk, D.J.; Emerson, R.H. Titanium as the material of choice for cementless femoral components in total hip arthroplasty. *Clin. Orthop. Relat. Res.* 1995, 311, 85–90.

60. Gibson, L.J.; Ashby, M.F. *Cellular Solids: Structure, Properties and Applications*; Cambridge University Press: Cambridge, UK, 2014; pp. 159–169.

61. Krishna, B.V.; Bose, S.; Bandyopadhyay, A. Low stiffness porous Ti structures for load-bearing implants. *Acta Biomater.* 2007, 3, 997–1006.

62. Hedia, H.S. Stress and strain distribution behavior in the bone due to the effect of cancellous bone, dental implant material and the bone height. *Bio-Med. Mater. Eng.* 2002, 12, 111–119.

63. Simon, U.; Augat, P.; Ignatius, A.; Claes, L. Influence of the stiffness of bone defect implants on the mechanical conditions at the interface—A finite element analysis with contact. *J. Biomech.* 2003, 36, 1079–1086.

64. Lei, S.; Lei, S.; Ling, W.; Yonghong, D.; Wei, L.; Zhen, W.; Jing, L.; Xiangli, F.; Xiaokang, L.; Shujun, L. The Improved Biological Performance of a Novel Low Elastic Modulus Implant. *PLoS ONE* 2013, 8, e55015.

65. Nune, K.C.; Misra, R.D.; Li, S.J.; Hao, Y.L.; Yang, R. Osteoblast cellular activity on low elastic modulus Ti-24Nb-4Zr-8Sn alloy. *Dent. Mater. Off. Publ. Acad. Dent. Mater.* 2017, 33, 152–165.

66. Li, K.; Li, M.; Zhao, Y.; Shan, W.; Cao, Y.; Guo, D. Achieving ultralow elastic modulus in TiNi alloy by controlling nanoscale martensite phase. *Mater. Lett.* 2018, 233, 282–285.

67. Mazigi, O.; Kannan, M.B.; Xu, J.; Choe, H.C.; Ye, Q. Biocompatibility and degradation of a low elastic modulus Ti-35Nb-3Zr alloy: Nanosurface engineering for enhanced degradation resistance. *ACS Biomater. Sci. Eng.* 2017, 3, 509–517.

68. Baragetti, S.; Arcieri, E.V. Corrosion fatigue behavior of Ti-6Al-4 V: Chemical and mechanical driving forces. *Int. J. Fatigue* 2018, 112, 301–307.

69. Songür, M.; Çelikkan, H.; Gökmeşe, F.; Şimşek, S.A.; Altun, N.Ş.; Aksu, M.L. Electrochemical corrosion properties of metal alloys used in orthopaedic implants. *J. Appl. Electrochem.* 2009, 39, 1259.

70. Lavenus, S.; Ricquier, J.C.; Louarn, G.; Layrolle, P. Cell interaction with nanopatterned surface of implants. *Nanomedicine (Lond)* 2010, 5, 937–947.

71. Fleck, C.; Eifler, D. Corrosion, fatigue and corrosion fatigue behaviour of metal implant materials, especially titanium alloys. *Int. J. Fatigue* 2010, 32, 929–935.

72. Al-Saffar, N.; Kadoya, Y.; Revell, P. The role of newly formed vessels and cell adhesion molecules in the tissue response to wear products from orthopaedic implants. *J Mater. Sci. Mater. Med.* 1994, 5, 813–818.

73. Al-Saffar, N.; Revell, P.A.; Kobayashi, A. Modulation of the phenotypic and functional properties of phagocytic macrophages by wear particles from orthopaedic implants. *J Mater. Sci. Mater. Med.* 1997, 8, 641–648.

74. Oliveira, M.N.; Schunemann, W.V.H.; Mathew, M.T.; Henriques, B.; Magini, R.S.; Teughels, W.; Souza, J.C.M. Can degradation products released from dental implants affect peri-implant tissues? *J. Periodont. Res.* 2018, 53, 1–11.

75. Vasudevan, A.K.; Sadananda, K. Classification of environmentally assisted fatigue crack growth behavior. *Int. J. Fatigue* 2009, 31, 1696–1708.

76. Metikoš-Huković, M.; Katić, J.; Grubač, Z.; Škugor Rončević, I. Electrochemistry of CoCrMo Implant in Hanks' Solution and Mott-Schottky Probe of Alloy's Passive Films. *Corrosion* 2017, 73, 1401–1412.

77. Okazaki, Y.; Nagata, H. Comparisons of immersion and electrochemical properties of highly biocompatible Ti–15Zr–4Nb–4Ta alloy and other implantable metals for orthopedic implants. *Sci. Technol. Adv. Mater.* 2012, 13, 064216.

78. Major, S.; Cyrus, P.; Hubálovská, M. The Influence of Surface Roughness on Biocompatibility and Fatigue Life of Titanium Based Alloys. *IOP Conf. Ser. Mater. Sci. Eng.* 2017, 175, 012053.

79. Sivakumar, B.; Kumar, S.; Narayanan, T.S.N.S. Comparison of fretting corrosion behaviour of Ti–6Al–4V alloy and CP-Ti in Ringer's solution. *Tribol. Mater. Surf. Interfaces* 2011, 5, 158–164.

80. Sommer, U.; Laurich, S.; de Azevedo, L.; Viehoff, K.; Wenisch, S.; Thormann, U.; Alt, V.; Heiss, C.; Schnettler, R. In Vitro and In Vivo Biocompatibility Studies of a Cast and Coated Titanium Alloy. *Molecules* 2020, 25, 3399.

81. Kaczmarek, M. Investigation of pitting and crevice corrosion resistance of NiTi alloy by means of electrochemical methods. *Prz Elektrotech.* 2010, 86, 102–105.

82. Atapour, M.; Pilchak, A.L.; Frankel, G.S.; Williams, J.C. Corrosion behavior of  $\beta$  titanium alloys for biomedical applications. *Mater. Sci. Eng. C* 2011, 31, 885–891.

83. Jesus, J.S.; Borrego, L.P.; Ferreira, J.A.M.; Costa, J.D.; Capela, C. Fatigue crack growth under corrosive environments of Ti-6Al-4V specimens produced by SLM. *Eng. Fail. Anal.* 2020, 118, 104852.

---

84. Slámečka, K.; Pokluda, J.; Kianicová, M.; Major, T.; Dvořák, I. Quantitative fractography of fish-eye crack formation under bending–torsion fatigue. *Int. J. Fatigue* 2010, 32, 921–928.

85. Navarro, C.; Vázquez, J.; Domínguez, J. A general model to estimate life in notches and fretting fatigue. *Eng. Fract. Mech.* 2011, 78, 1590–1601.

---

Retrieved from <https://encyclopedia.pub/entry/history/show/15400>